Validation of the 4C Thermal-Hydraulic Code Against 25 kA Safety Discharge in the ITER Toroidal Field Model Coil (TFMC)

R. Zanino, R. Bonifetto, R. Heller, and L. Savoldi Richard

***Abstract*—The first step of the validation of the recently developed thermal-hydraulic code 4C is presented. We study the transient evolution during a so-called standard 25 kA safety discharge of the International Thermonuclear Experimental Reactor (ITER) Toroidal Field Model Coil (TFMC), tested in 2001–2002 in the TOSKA facility at the Karlsruhe Institute of Technology, Germany. The computed outlet He temperatures from both winding and case cooling channels, as well as the local maximum temperature increase of the structures, are shown to be in good agreement with the measured data.**

***Index Terms*—Fusion reactors, simulation, superconducting coils.**

I. Introduction

THE 4C code [1] was recently developed for the coupled simulation of thermal-hydraulic (TH) transients in the superconducting coils and related cryogenic circuit of the International Thermonuclear Experimental Reactor (ITER). The code combines a detailed 1D description of the compressible flow of the supercritical He coolant along each conductor in the winding, with a 3D model of heat transfer in the solid structures and a 0D–1D model of the cryogenic circuit (including pumps, valves, cryolines, heat exchanger). A first realistic, predictive application of the 4C code to the quench simulation of an ITER Toroidal Field coil was recently published [2].

In this paper we present the first step of the 4C validation, against the database collected in 2001–2002 during the test of the ITER Toroidal Field Model Coil (TFMC) in the TOSKA facility at the Karlsruhe Institute of Technology (which is a merger of the Forschungszentrum Karlsruhe and the University of Karlsruhe), in Germany [3]. A safety discharge of the TFMC from 25 kA is simulated with 4C, accounting for the time dependent heat deposition in the conductors, radial plates and coil case. The resulting TH evolution of the system is then compared with the experimental results.

Manuscript received August 03, 2010; accepted October 15, 2010.

R. Zanino, R. Bonifetto, and L. Savoldi Richard are with Dipartimento di Energetica, Politecnico di Torino, 10129 Torino, Italy (e-mail: roberto.zanino@polito.it).

R. Heller is with Institut fuer Technische Physik, Karlsruhe Institute of Technology, 76344 Eggenstein-Leopoldshafen, Germany (e-mail: reinhard.heller@kit.edu).

Color versions of one or more of the figures in this paper are available online at http://ieeexplore.ieee.org.

Digital Object Identifier 10.1109/TASC.2010.2089771

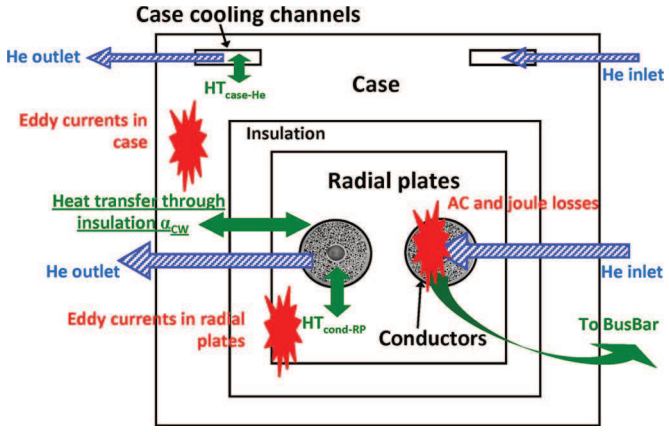

Fig. 1. Schematics of the system studied in the present paper: stars = heat sources, dashed arrows = helium flows, solid arrows = heat transfer channels.

II. Problem Definition

The TFMC was a racetrack Nb3Sn coil with circular dual channel conductors pancake-wound into the grooves of stainless steel radial plates (RP); the suitably insulated winding (conductors + RP) was then enclosed in a separately cooled, stainless steel case. Structures (RP + case) account for ~80% of the total mass of the coil and ~25% of the heat capacity at the nominal operating temperature of 4.5 K.

During the TFMC test a so-called standard safety discharge from 25 kA was used to evaluate AC losses: the coil is discharged with an exponential time constant and this causes a heat load on the coil, due to AC losses in the conductors as well as eddy current dissipation in the radial plates and the coil case, which drives the TH transient (in the experiment, the initial current was chosen below the maximum TFMC current of 80 kA in order to minimize the impact of the discharge on the cryogenic system).

From the point of view of the modeler, it is first of all important to properly identify the system to be studied. In the case at hand, see Fig. 1, some specific items are highly relevant and are therefore discussed below in detail, namely: 1) the geometry and operating conditions of winding and case cooling circuits, 2) the heat sources acting on the coil, 3) the transport coefficients (friction factors, heat transfer coefficients) needed for the description of the interactions between different coil components, 4) the initial and the boundary conditions. Provided all of the above (input) ingredients are adequate, a comparison with the

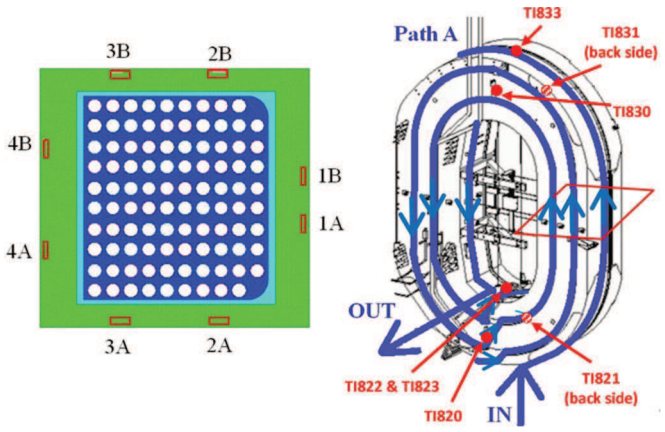

Fig. 2. Left: cross section of the TFMC case (highlighted on the right and seen from above) with rectangular cooling channels; the two parallel paths A and B are highlighted, the numbering refers to the ordering of the channels in the hydraulic series; the inner side of the coil is on the left of the figure (channels 4A, 4B). Right: 3D view of the TFMC with corresponding cooling path of circuit A and relevant case temperature sensors locations.

experiment allows an assessment of the quality and accuracy (i.e., a validation) of the model presently implemented in 4C.

A. Winding and Case Cooling Circuits

The layout of the TFMC winding and of the respective cooling circuit is shown in [3], Figs. 3.1 and 3.13, respectively. For our present purpose, the most important features are as follows: 1) the coil is wound in five double pancakes, with single pancakes, hydraulically in parallel, identified as P1.1, P1.2, . . ., P5.2; 2) the He inlet is on the inner mid-plane side of the (racetrack shaped) coil; 3) the total He mass flow rate is measured only at the inlet (FI700) and includes the He mass flow rate in the bus bars (BB), which is estimated to be ∼20% of the total; 4) the measured global outlet temperature TI701 refers to the mixing of outlet temperature of the 10 pancakes only, excluding BB (several other outlet temperatures are measured, see below, pertaining to single pancakes or pairs of pancakes).

The case cooling circuit is made of two parallel paths, each consisting of four channels in series with roughly rectangular cross section of $\sim 32 \times 5\ \mathrm{mm}^2$, see Fig. 2.

B. Heat Sources

The heat source P_{tot} which drives the TH transient studied in the present paper is defined in [3] and is related to the presence of the transport current (Joule losses P_{J} in the joints and so-called power supply ripple losses P_{ripple} in the radial plates [3]), and to the variation of this current in time (hysteresis and coupling losses P_{hyst} and P_{coupl} in the conductors, eddy current losses $P_{\mathrm{eddy,wind}}$, $P_{\mathrm{eddy,case}}$ in the radial plates and the case respectively). Concerning the second group, and in particular $P_{\mathrm{eddy,wind}}$ and $P_{\mathrm{eddy,case}}$, not enough information is available to assess the spatial distribution of the sources, which will be therefore assumed as uniform.

The correct use of these sources requires some caution. Let us start by applying the first principle of thermodynamics to the entire coil. Integrating over the whole transient we get

$$U(t_{end}) - U(0) = \int_0^{t_{end}} P_{tot}(t)dt - \int_0^{t_{end}} Q_{BB}(t)dt - \int_0^{t_{end}} \sum \left[\Gamma_{out}(t)h_{out}(t) - \Gamma_{in}(t)h_{in}(t)\right] dt \quad (1)$$

where U is the internal energy (J), the origin of the time coordinate t (s) has been set at the moment of the current dump, P_{tot} is the total heat generation (W), Q_{BB} is the heat (W) transferred by conduction through the joint between P1.1 or P5.2 and the respective BB, Γ is the He mass flow rate (kg/s), h is the specific enthalpy (J/kg), indexes "in" and "out" refer to inlet and outlet cross section, respectively, and the sum adds the contributions of winding and case cooling.

In order to calibrate ad hoc the coefficients present in the formulas [3] for the different contributions to P_{tot}, several simplifying assumptions were made in [3], including: 1) $U(t_{\mathrm{end}}) \approx U(0)$, as $U(0) - U(t_{\mathrm{end}})$ can be estimated as $\leq$30 kJ, based on the difference between initial and final steady state outlet He temperatures, due in turn to $P_{\mathrm{J}} + P_{\mathrm{ripple}}$; 2) $\Gamma_{\mathrm{out}} \approx \Gamma_{\mathrm{in}}$, since only Γ_{in} was measured, while simulations show that the two can be significantly different during the transient, see below; 3) offset of the virtual signals QMFI700 and QMFI800 providing the enthalpy power integrands for winding and case, respectively, with respect to their final values, assuming this offset as due to steady state heat loads (conduction, radiation), which are not considered in the energy balance; 4) nominal current decay time constant $\tau_{\mathrm{dump}} = 4$ s, instead of the actual measured one ∼3.55 s, see [3], Fig. 6.17.

Under these assumptions, the total energy deposited in the coil during the 25 kA safety discharge can be estimated by the formulas given in [3] as ∼400 kJ, of which ∼60% are deposited in the winding. It should be noted, however, that while the total energies are reliable, the single contributions of RP, case, etc, cannot be separately checked because these subsystems are thermally coupled.

Here we shall consistently adopt the above-mentioned assumptions 1, 3 and 4, while the heat source will be iteratively adapted, in order to comply with $\Delta\Gamma, \Delta U \neq 0$: at convergence of the iterations a reduction of the total energy by a factor of typically ∼0.8 results, and a corresponding reduction is applied to P_{hyst}, P_{coupl}, $P_{\mathrm{eddy,wind}}$ and $P_{\mathrm{eddy,case}}$, with respect to their nominal values.

C. Transport Coefficients

The transport coefficients which need to be defined include the friction factors for the He flow in the different conductors and channels and the heat transfer coefficients between the different coil components.

Concerning friction factors, in the winding the Katheder correlation has been used for the cable bundle region, with a multiplier of 1.5, whereas for the central channel the correlation

TABLE I
THERMO-PHYSICAL PROPERTIES OF THE MATERIALS AT 4.5 K

Property	Cu	Nb_3Sn	SS	EP	GE
ρ (kg/m^3)	8900	8950	7800	1700	2000
cp (J/kgK)	0.117	0.218	2.12	1.15	0.517
k (W/mK)	698	0.0549	0.267	0.0504	0.0634

proposed in [4] has been used, which already accounts for the different types of spirals used in different TFMC pancakes; this combination of choices was shown in [5] to reproduce very accurately the hydraulic characteristic of both P1.1 and P1.2. For the case cooling channels, the correlation for smooth rectangular ducts given in [6] has been used.

As to the heat transfer coefficients: between the conductor and the radial plates, $\sim 5\ \mathrm{W/m^2\ K}$ is obtained from the thermal resistance of the 2.5 mm impregnated turn insulation, multiplied by a factor ∼6 as recommended in [3], [7]; between the He flowing in the case cooling channels and the case a value of $\sim 150-200\ \mathrm{W/m^2\ K}$ is obtained from correlations for rectangular ducts heated on 2–4 sides [6], respectively, which led us to assume $\sim 100\ \mathrm{W/m^2\ K}$ in our case, where the channel is mainly heated only on 1 side. The case-RP interface, i.e., the ground insulation, has a finite thickness discretized by 4C and heat transfer there is modeled by assuming, for the mixture of glass Kapton and silica sand, impregnated with epoxy resin, a single heat diffusivity $\alpha_{\mathrm{CW}} = \alpha_{\mathrm{epoxy}}$. Transport properties used in this paper are temperature dependent; some relevant values at 4.5 K are given in Table I.

D. Initial and Boundary Conditions

Boundary conditions for the He prescribe measured inlet temperature $T_{\mathrm{in}}(t)$ and speed $V_{\mathrm{in}}(t)$, together with the measured outlet pressure $p_{\mathrm{out}}(t)$ for the different pancakes and the case cooling channels (V_{in} is used instead of the more customary inlet pressure $\mathrm{p_{in}(t)}$ because the accuracy of $p_{\mathrm{in}}(t) - p_{\mathrm{out}}(t)$ is not sufficient to carefully compute Γ; V_{in} is deduced from measured Γ_{in} and inlet density computed from measured $p_{\mathrm{in}}(t)$, $T_{\mathrm{in}}(t)$). These data are acquired in the experiment with a 5 s sampling period; therefore the very initial heat deposition phase of the transient may not be accurately reproduced. Note also that the availability of measured boundary values makes it unnecessary to include the external cryogenic circuit in the model, while the opposite is true in the case of predictive applications, e.g. [2]. Concerning the solids, the only boundary condition needed is at the case outer boundary, which is assumed to be adiabatic.

The initial conditions are obtained by running the code until steady state is reached taking into account only those sources acting on the coil which are relevant before the current dump was started, namely P_{J} and $P_{\mathrm{ripple}} \sim 40$ W [3].

III. 4C COMPUTATIONAL MODEL

The winding model includes the 1D compressible He flow in the central channel and the cable region for each of the 10 pancakes in hydraulically parallel channels, 9 or 10 turns each depending on the pancake, coupled to heat conduction along the cable and the jacket and thermally coupled to the RPs.

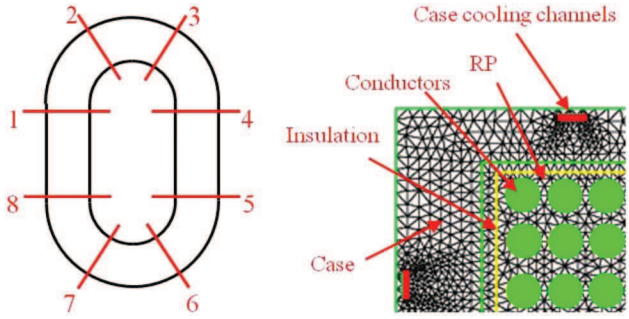

Fig. 3. Left: poloidal distribution and numbering of cuts in the case $N = 8$. Right: zoom on a cut, showing the finite element triangulation of the structures and the different coil components included in the model.

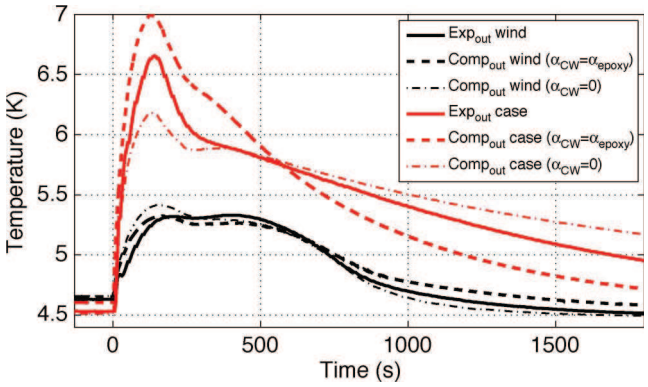

Fig. 4. Comparison between computed (dashed: $\alpha_{\mathrm{CW}} = \alpha_{\mathrm{epoxy}}$, dash-dotted: $\alpha_{\mathrm{CW}} = 0$) and measured (solid) He temperatures evolution at the winding (black) and case (red) outlet manifolds.

The case cooling channels model includes the 1D compressible He flow thermally coupled to the case.

The 3D heat transfer problem in RPs and case is approximated with N cuts, regularly distributed in the poloidal direction (along the racetrack), see Fig. 3; on each cut the 2D heat conduction problem is solved by finite element methods, see Fig. 3. Since the poloidal heat conduction timescale through the structures is orders of magnitude longer than the helium transit time (along the same poloidal distance), the cuts are coupled to each other only by helium advection in the pancakes, while heat conduction in the structures is neglected in the poloidal direction. The results presented here refer to the case $N = 8$, the grid independence of the solution was demonstrated running the code with $N = 4$.

IV. RESULTS

We consider here in detail the 25 kA safety discharge performed on 26/09/2001, whose results were shown to be fully reproducible in other discharges [3]. Arguably, the most important feature of the whole transient is the evolution of the He outlet temperatures shown in Fig. 4. Since the time for heat deposition is very short (few s), T_{out} reaches a maximum on a time scale of the order of the He transit time (∼150–200 s) both in the winding and in the case, in the former depending on the assumed value for the thermal resistance of the turn insulation, see Section II-C. Then T_{out} starts decreasing until a second structure appears, either in the form of a minimum (as

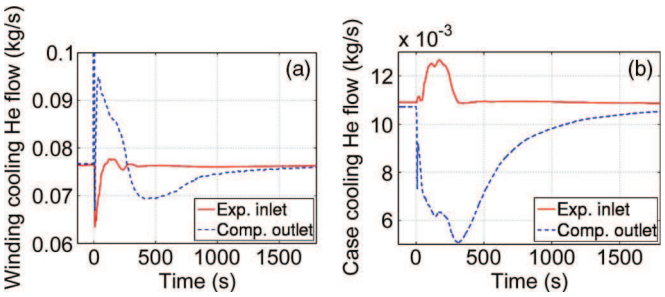

Fig. 5. Measured inlet total mass flow rates (used as boundary conditions) and correspondingly computed total outlet mass flow rates. (a) Winding and (b) Case.

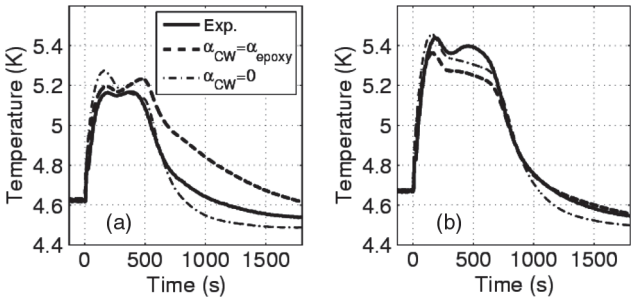

Fig. 6. Comparison between computed (dashed: $\alpha_{\mathrm{CW}} = \alpha_{\mathrm{epoxy}}$, dash-dotted: $\alpha_{\mathrm{CW}} = 0$) and measured (solid) He temperatures evolution. (a) P1.1 and (b) P3.2&P4.1.

in the winding), or in the form of a marked change of slope or "knee" (as in the case cooling channels). This second feature is quite clearly synchronized with the more-or-less sudden decrease of Γ_{out}, as shown in Fig. 5. Indeed, the corresponding reduced cooling efficiency leads to a second peak in the winding because, in view of the weak thermal coupling to the RPs, they still have to release most of the accumulated heat. On the contrary, in the case cooling channels, where the He is relatively well thermally coupled to the case, a clear maximum does not appear and T_{out} continues decreasing.

All of the above-mentioned qualitative features are well reproduced by the simulation. The computed results are also in very good quantitative agreement with the experiment in the case of the winding, whereas the case cooling channel peak is somewhat overestimated by the code, as well as the slope after the knee. This discrepancy is probably due to the fact that the diffusivity α_{CW} of the case-winding interface is overestimated. Indeed, assuming $\alpha_{\mathrm{CW}} = 0$ provides a nice bracketing of the measured evolution, see Fig. 4.

The evolution of the measured inlet mass flow rates Γ_{in} shown in Fig. 5 for both the winding and the case can be qualitatively explained as follows (a full quantitative explanation should require modeling the whole cryogenic circuit, which is beyond the scope of the present paper): Γ_{in} is suddenly reduced in the winding because the sudden deposition of heat in the conductors leads to pressurization of the He; since winding and case cooling channels are in parallel and both fed by a piston pump with an almost vertical characteristic, such that the total mass flow rate cannot vary too much, the decrease of Γ_{in} in the winding is accompanied by an increase of Γ_{in} in the case cooling channels.

As to the evolution of the computed outlet mass flow rates Γ_{out}, also shown in Fig. 5, it can be seen that the behavior of the winding and of the case is again opposed: while in the winding the sudden pressurization leads to a sudden increase of Γ_{out}, it is seen that Γ_{out} in the case decreases after the dump and this is due to the fact that the warm temperature front is being advected along the case cooling channels carrying He with lower density and therefore reduced mass flow rate even at almost constant speed.

In Fig. 6 the He outlet temperatures from an outer pancake (P1.1) and from an inner pair of pancakes (P3.2&P4.1) are presented. Outer pancakes, thermally coupled with the case and with the BBs, reach lower peak temperatures. The simulation results are in good qualitative agreement with the experiment,

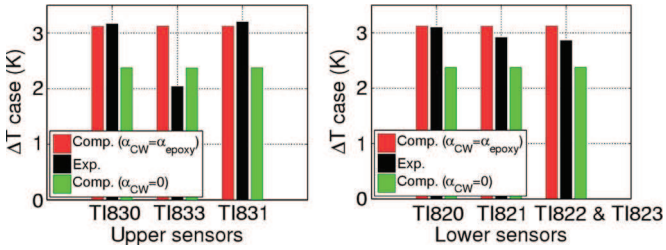

Fig. 7. Comparison between computed (red: $\alpha_{\mathrm{CW}} = \alpha_{\mathrm{epoxy}}$, green: $\alpha_{\mathrm{CW}} = 0$) and measured (black) maximum temperature increase at different case temperature sensor locations. The corresponding sensor names are given on the x axis.

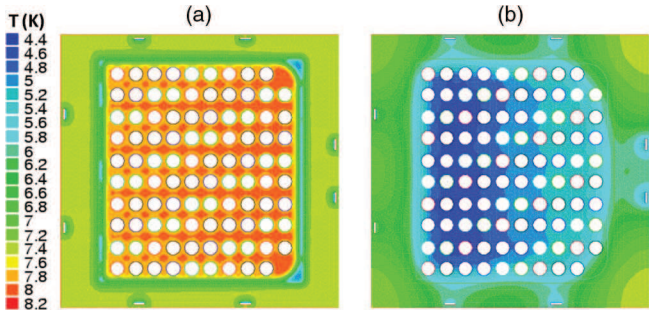

Fig. 8. Computed temperature distributions on a structure cut: (a) $t = 5$ s, (b) $t = 400$ s.

and the sensitivity to α_{CW} provides again a nice quantitative bracketing, in particular for the outer pancakes in direct contact with the case (Fig. 7).

The TFMC case was instrumented with several temperature sensors, the most relevant of which are shown in Fig. 2, located either in the top region of the coil (left figure) or in the bottom region (right figure), on different coil sides. Also here the simulation is able to closely reproduce the measured results.

The temperature distributions computed in the structures at two different times are shown in Fig. 8. In the very first phase of the transient (i.e., during heat deposition), the heat transfer between the case and the RPs is sufficiently weak to allow building up a gradient: the RPs are warmer because of the higher input power and the insulation between the two is cold as no sources act on it. On the longer timescale several combined phenomena occur: the heat transfer between the different coil components is now effective, so that gradients between RP and case tend

to disappear, whereas the action of the helium coolant is highlighted both in the case and in the winding: in the former, temperature gradients arise because of the localized nature of the case cooling channels; in the latter, the advancing cold front advected along the pancakes produces a temperature gradient across turns.

V. Conclusions and Perspective

The first complete thermal-hydraulic simulation of a TFMC standard safety discharge from 25 kA has been presented.

The 4C code has been shown to be able to quantitatively reproduce with good accuracy the measured He outlet temperature evolution from the winding as well as the measured local maximum case temperature increase; the key qualitative features of the measured evolution of the He outlet temperature from the case are also reproduced by the simulations, while sensitivity to the uncertain value of the heat diffusivity of the insulation between case and winding was shown to provide a quantitative bracketing.

Within the framework of a continuing validation plan of 4C, the analysis of the cool-down of a W7-X Non-Planar Coil during its cold test has been presented elsewhere [8], [9].

References

[1] L. Savoldi Richard, F. Casella, B. Fiori, and R. Zanino, "The 4C code for the cryogenic circuit conductor and coil modeling in ITER," *Cryogenics*, vol. 50, pp. 167–176, 2010.

[2] R. Zanino, D. Bessette, and L. Savoldi Richard, "Quench analysis of an ITER TF coil," *Fus. Eng. Des.*, vol. 85, pp. 752–760, 2010.

[3] A. Ulbricht *et al.*, "The ITER toroidal field model coil project," *Fus. Eng. Des.*, vol. 73, pp. 189–327, 2005.

[4] R. Zanino, P. Santagati, L. Savoldi, A. Martinez, and S. Nicollet, "Friction factor correlation with application to the central cooling channel of cable-in-conduit super-conductors for fusion magnets," *IEEE Trans. Appl. Supercond.*, vol. 10, pp. 1066–1069, 2000.

[5] L. Savoldi Richard and R. Zanino, "Correlazioni per fattori d'attrito nei cavi superconduttori di ITER," *Atti del 58 ^{circ} Congresso annuale dell'ATI*, pp. 2213–2224, 2003.

[6] S. Kakac, R. K. Shah, and W. Aung, *Handbook of Single-Phase Convective Heat Transfer*. New York: Wiley , 1987.

[7] J. L. Duchateau *et al.*, "ITER toroidal field model coil test: Analysis of heat transfer from plates to conductors," *Fus. Eng. Des.*, vol. 66–68, pp. 1007–1011, 2003.

[8] R. Bonifetto, A. Kholia, B. Renard, K. Risse, L. Savoldi Richard, and R. Zanino, "Modeling of W7-X superconducting coil cooldown using the 4C codet," presented at the Symposium on Fusion Technology, Porto, 2010.

[9] R. Bonifetto, A. Kholia, B. Renard, K. Risse, L. Savoldi Richard, and R. Zanino, "Modeling of W7-X superconducting coil cooldown using the 4C codet," *Fus. Eng. Des.*, 2010, submitted for publication.